Solid State Sciences 13 (2011) 1047–1051

Contents lists available at ScienceDirect

Solid State Sciences

journal homepage: www.elsevier.com/locate/ssscie

Improved performance of polyvinylidenefluoride–hexafluoropropylene based nanocomposite polymer membranes containing lithium bis(oxalato)borate by phase inversion for lithium batteries

V. Aravindan [a,b], P. Vickraman [a,*], S. Madhavi [b,c], A. Sivashanmugam [d], R. Thirunakaran [d], S. Gopukumar [d]

[a] Department of Physics, Gandhigram Rural University, Gandhigram 624 302, India
[b] Energy Research Institute, Nanyang Technological University, Research Techno Plaza, 50 Nanyang Drive, Singapore 637553, Singapore
[c] School of Materials Science and Engineering, Nanyang Technological University, Singapore 639798, Singapore
[d] Electrochemical Energy Systems Division, Central Electrochemical Research Institute, Karaikudi 630 006, India

ARTICLE INFO

Article history:
Received 23 April 2010
Received in revised form
12 January 2011
Accepted 28 January 2011
Available online 4 February 2011

Keywords:
LiBOB
Nanocomposite
PVdF–HFP
Lithium batteries

ABSTRACT

Nanocomposite polymer electrolyte membranes were prepared by phase inversion technique in polyvinylidenefluoride–hexafluoropropylene (PVdF–HFP) matrix. These membranes were gelled with 0.5 M LiBOB in EC:DEC (1:1 v/v). These gel polymer membranes (GPMs) were incorporated with nanoparticles of $AlO(OH)_n$ and prepared composite polymer membranes (CPMs) also. The a.c. impedance analysis shows that $AlO(OH)_n$ filled membrane exhibits conductivity of 1.82×10^{-3} S cm^{-1} at ambient temperature. The Li/CPM/$LiFePO_4$ cell delivered a specific discharge capacity of 158 and 147 mAh g^{-1} at first and at 20th cycle respectively discharged at C/20 rate. The cell experiences a capacity fade of 0.1 mAh g^{-1} cycle^{-1} over the investigated 20 cycles. The studies vindicate that $AlO(OH)_n$ filled PVdF–HFP polymer membranes could be the potential material to use as separator cum electrolyte in lithium batteries in conjunction with $LiFePO_4$ as a counterpart.

1. Introduction

Of late, an increasing interest is being devoted towards the development of polymer electrolyte membranes for lithium rechargeable batteries with improved ionic conductivity, mechanical, electrochemical and thermal stabilities. Porosity is also one of the basic requisites envisaged for polymer electrolyte membranes to allow the Li^+ ions to transit between the anode and cathode during charging and discharging. Tarascon et al. [1] pioneered the preparation of porous membranes by a two-step process with/without SiO_2 fillers by varying hexafluoropropylene (HFP) units in polyvinylidenefluoride (PVdF) in the first step and in the second step extraction of di-butyl phthalate (DBP) was found to be very difficult and enhances production cost.

The phase inversion technique [2] has been adopted for preparing polymer membranes without sacrificing the basic requisites with optimized solvent/non-solvent ratio and effectively controlling the pore size distributions. Recent investigations identify that the addition of nano-sized ceramic oxides substantially increases the conductivity [2–6], Li^+ transference number, mechanical, thermal and electrochemical stabilities. In this line numerous investigations were reported [2,7–9] based on SiO_2, TiO_2, Al_2O_3, etc. as fillers, which guarantee superior properties to the polymer membranes as their surface exists either as acidic or basic or a mixture of these two. These surfaces effectively interact with the polymer chains and preventing their reorganization resulting in the formation of more amorphous domain in the host [2–9].

Yu et al. [10] investigated the LiBOB based polymer electrolytes for lithium batteries with various cathode materials for the first time and discharge capacities of 132.6, 113.6 and 160 mAh g^{-1} were obtained for $LiCoO_2$, $LiMn_2O_4$ and $LiNi_{1/3}Co_{1/3}Mn_{1/3}O_2$ materials respectively. Dahn and co-workers [11] have reported the severe interaction of lithium bis(oxalato)borate (LiBOB) based electrolytes with these cathode materials except $LiFePO_4$ by accelerating rate calorimetric studies however, a thorough electrochemical cycling study using $LiFePO_4$ as a cathode material has not been extensively studied. In this context, the present investigation is envisaged to explore the possibility of using polyvinylidenefluoride–hexafluoropropylene (PVdF–HFP) based polymeric membranes with and without $AlO(OH)_n$ nanoparticles gelled with LiBOB in ethylene carbonate (EC)/diethyl carbonate (DEC) in conjunction with $LiFePO_4$ as cathode material.

* Corresponding author. Tel.: +91 451 2452371; fax: +91 451 2454466.
E-mail addresses: aravind_van@yahoo.com (V. Aravindan), vrsvickraman@yahoo.com (P. Vickraman).

1293-2558/$ – see front matter © 2011 Elsevier Masson SAS. All rights reserved.
doi:10.1016/j.solidstatesciences.2011.01.022

2. Materials and methods

2.1. Chemicals

Very high molecular weight PVdF–HFP with 12 mol% of HFP (Solvay Solexis, Italy, Mw 5.34×10^5), lithium hydroxide monohydrate (Aldrich, USA); $AlO(OH)_n$ (Candia, Taiwan with the size of 14 nm); $LiFePO_4$ (Hydro Quebec, Canada), ethylene carbonate, diethyl carbonate, acetone, ethanol and *n*-butanol (E. Merck, India) were used as received.

2.2. Synthesis of LiBOB

LiBOB was synthesized by solid-state method [10,12] according to the reaction shown in Scheme 1. Oxalic acid dihydrate, lithium hydroxide, and boric acid were dissolved in triple distilled water in molar ratio of 2:1:1 using a blender for 1 min. The solution was annealed in an oven at 240 °C for 5 h to prepare LiBOB. The product was purified by dissolving in the boiling tetrahydrofuran/diethyl ether (1:1 molar ratio) and re-crystallizing at −25 °C. Subsequently, the sample was dried in vacuum at about 60 °C for 48 h [13–16].

2.3. Instrumentation

In the typical phase inversion technique, the polymer PVdF–HFP, is dissolved in a mixture of acetone (solvent) and ethanol (non-solvent) (5:1 volume ratio) with the proportion of the non-solvent low enough to allow dissociation and high enough to allow phase separation during evaporation. The non-solvent is to be fixed in such a way that it will have better porosity during the solvent evaporation process. The prepared solution is formed into thin films on a glass substrate, and the solvent is allowed to evaporate. The prepared films are kept under vacuum for 12 h at 100 °C to remove the traces of non-solvents. A similar procedure has been adopted for the composite membrane preparation and $AlO(OH)_n$ nanoparticles were introduced once the polymer dissolution occurs with the optimized concentration of 10 wt% [13]. Morphological features of the polymer membranes were examined using a Hitachi Model S-3000H scanning electron microscope (SEM). Ionic conductivities of the membranes were measured by a.c. impedance spectroscopy in the frequency range between 5 MHz and 1 Hz in a Solartron 1260 Impedance/Gain Phase Analyzer coupled with a Solartron Electrochemical Interface using a stainless steel blocking electrode impedance cell of 1 cm^2 area. Differential scanning calorimetric studies of the polymer membranes were recorded using a Perkin–Elmer Pyris 6 instrument under nitrogen atmosphere between 50 °C and 250 °C at a heating rate of 10 °C/min. Instron Corporation series IX automated mate has been used to measure the mechanical strength of the polymer membranes. The surface area and pore size of the membranes were determined by a continuous flow nitrogen gas adsorption/desorption BET apparatus (Gemini, Micromeritics, USA).

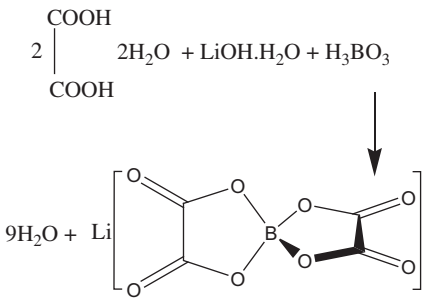

Scheme 1. Schematic representation of the synthesis of LiBOB.

2.4. Coin cell assembly

Coin cells of 2016 configuration were assembled using lithium metal as a anode, $LiFePO_4$ as a cathode and composite polymer membranes as separator cum electrolyte soaked in 0.5 M LiBOB in EC:DEC (1:1 v/v) for an hour. The $LiFePO_4$ cathodes were prepared by a slurry coating process over the aluminium foil using doctor blade comprising of $LiFePO_4$ (60%), carbon black (30%) and PVdF binder (10%). The *N*-methyl pyrrolidone (NMP) was used as slurrying agent. The coated aluminium foil was dried in an oven at 110 °C for 2 h and pressed and 18 mm diameter blanks were punched out from the coated area and used as cathode. Coin cells were assembled inside an argon filled glove box (M Braun, Germany) and subjected to electrochemical cycling studies. Cycling behaviour of Li/$LiFePO_4$ cells with polymer electrolyte membranes was performed galvanostatically in a computerized battery cycling unit at C/20 rate for the first cycle and the rest at C/10 rate between the potential windows 2.5–4.5 V.

3. Results and discussion

3.1. Thermal studies

Thermal stability is also vital to guarantee acceptable performance at elevated temperatures in addition to high ionic conductivity, high lithium ion transport number and good mechanical strength of the polymer membranes. Fig. 1 depicts the DSC traces of the bare, gel and composite PVdF–HFP membranes. In the case of bare PVdF–HFP membranes, endotherm observed at 137.03 °C is owed to the melting of dominant a crystalline phase of the polymer. Except bare membrane, rest of the two-gelled membranes exhibited the endotherm at around ~80–100 °C are ascribed to the removal of moisture during the loading of the sample. This is expected only, because lithium ion solvated EC:DEC solution having the tendency of absorbing moisture quickly in the atmosphere. For gel membranes (GPMs), this endotherm shifts towards the lower temperature (102.30 °C) and present as two stage events. In addition to that, gelling agents greatly reduce the melting temperature

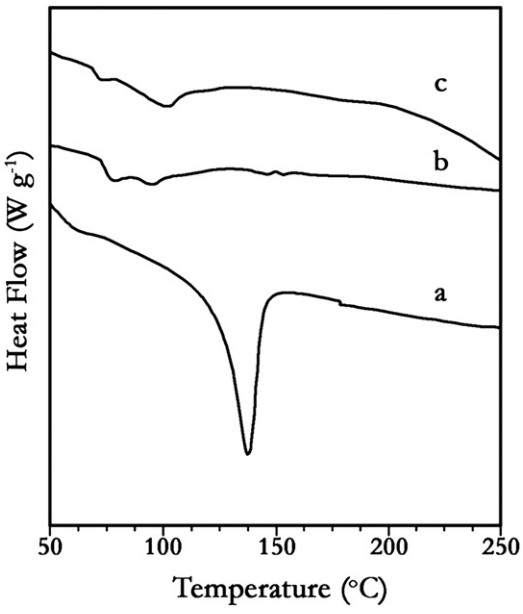

Fig. 1. Differential scanning calorimetric traces of (a) bare (b) gel and (c) composite PVdF–HFP membranes.

and its specific heat as shown in Fig. 1. This could be seen from the appearance of a shallow endotherm peak signature as compared to the well-defined sharp endotherm observed for bare PVdF–HFP membranes. As far as composite polymeric membrane (CPM) is concerned, the endotherm shifts slightly towards the higher temperature (109.16 °C) which may be ascribed to the addition of $AlO(OH)_n$ nanoparticles.

Percentage of crystallinity is calculated for the polymeric membranes using the relation $\chi_c = \Delta H_m/\Delta H_m^o$ where ΔH_m^o is the reference heat of fusion (104.7 J g^{-1}) for pure a-phase crystals of PVdF–HFP and ΔH_m is the heat of fusion. Naturally, a-phase crystals are bound higher content in PVdF–HFP than β, γ and δ phases. The areas of high-temperature melting endotherm give the melting enthalpy of the polymer crystalline phase, ΔH_m. In the limits of the experimental errors, the amount of this phase was not influenced by the solution content. Crystallinity of 27.88%, 16% and 14% is obtained for pure PVdF–HFP, GPM and CPM respectively. This crystallinity calculation reveals that addition of nanoparticles effectively prevents the reorganization of polymer chains which leads to the decrease in crystallinity [17,18].

3.2. Mechanical stability

Addition of inorganic fillers into the polymer matrix is found to enhance mechanical properties of the host materials [19–22]. This enhancement is achieved by maximizing the interaction between the polymer matrix and filler particles [19–21]. Consequently a smaller filler particle presents larger active surface area for interaction with the polymer host. Such a simple inclusion of nano-fillers would also be beneficial to derive polymer membranes with pleasing mechanical strength. In the present investigation, tensile test of bare, GPM and CPM membranes is carried out and the stress–strain behaviour is depicted in Fig. 2.

It could be seen that, after gellation the polymeric membranes show Young's modulus around 4.13 MPa, while the elongation break is 122, 349 and 506% for bare PVdF–HFP, GPM and CPM respectively. The incorporation of 10% $AlO(OH)_n$ in the polymer membrane results in a drastic enhancement in their mechanical stability (CPM exhibits elongation break value 144 and 414% which are higher than the GPM and bare PVdF–HFP). It is inferred that the improved mechanical properties may be ascribed to the high mobility of $AlO(OH)_n$ nanoparticles under applied stress helping of dissipation of energy. Gersappe [22] showed by molecular simulations of polymers reinforced with nanoparticles that, it is the mobility of the nano-filler particles that controls the ability to dissipate energy rather than the surface area, resulting in an improved toughness of the composite material. A similar type of improvement is observed while investigating the effect of layered SiO_2 nano-sized particles in PVdF and polystyrene polymer hosts by Shah et al. [23,24].

3.3. Ionic conductivity

Ionic conductivity of polymer membranes were measured at ambient and elevated temperatures viz., 40, 50, 60 and 70 °C using impedance spectroscopy from the following equation:

$$\sigma = \frac{l}{R_b r^2 \pi} \quad (1)$$

where l and r represent thickness and radius of the sample membrane disk respectively. R_b is the bulk resistance obtained from a.c. impedance measurements. The conductivities of gel (GPM) and composite PVdF–HFP membranes are 5.23×10^{-4} and 1.82×10^{-3} S cm^{-1} respectively. It is clearly seen that, addition of nano-particulate $AlO(OH)_n$ substantially enhances the conductivity.

The enhancement of conductivity may be attributed to the Lewis acid–base interaction between the OH^- groups of the nano-particulate $AlO(OH)_n$ and F atoms of the polymer molecules, which prevents the reorganization of polymer chains making vast amorphous domain resulted in higher electrolyte uptake than GPM at ambient temperature conditions [17]. The aforementioned interaction promotes the dissociation of salts via the sort of "ion–filler" complex formation [25]. The temperature dependence of the ionic conductivity is depicted in Fig. 3. It can be seen that the conductivity of the films increases with increase in temperature. As the temperature increases, the polymer expands easily and produces free volume which in turn facilitates free mobility of ions with in the polymer network resulting to an increase in conductivity [12]. The similar trend has been observed by Stephan et al. [26] while incorporating different sizes (nano and micro) of $AlO(OH)_n$ particles in PVdF–HFP matrix using $LiN(CF_3CF_2SO_2)_2$ or $LiClO_4$ salt.

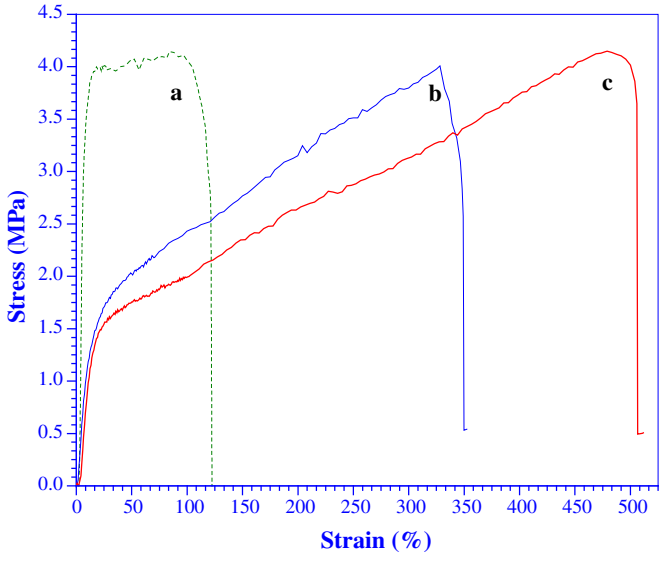

Fig. 2. Stress–strain curves of (a) bare (b) gel and (c) composite PVdF–HFP polymeric membranes.

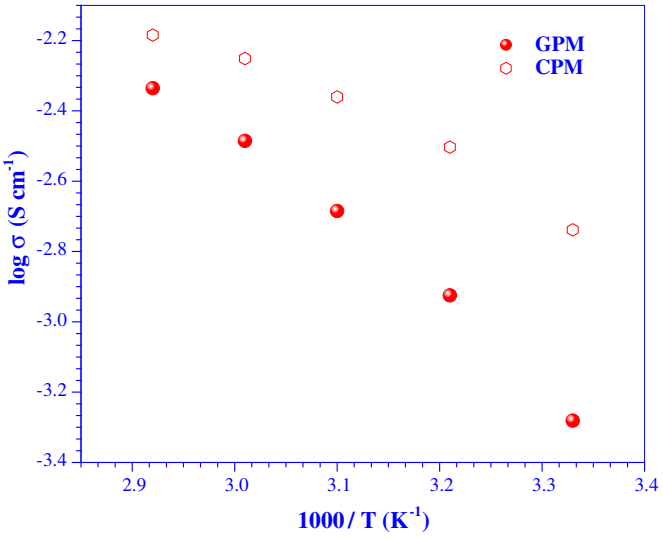

Fig. 3. Temperature dependence of ionic conductivity of the polymeric membranes.

3.4. Physical properties

The various physical properties of the gel and composite PVdF–HFP membranes are summarized in Table 1 and the calculations are made according to Li et al. [17] are given below.

$$\text{Electrolyte uptake}\ (\%) = \frac{W - W_o}{W_o} \times 100 \quad (2)$$

where W and W_o are the weights of wet and dry membranes respectively.

$$\text{Porosity of the membrane}\ p = \frac{\left(\frac{m_a}{\rho_a}\right)}{\left(\frac{m_a}{\rho_a} + \frac{m_p}{\rho_p}\right)} \quad (3)$$

where m_a, m_p are the masses of wet and dry membranes and r_a, r_p are density of *n*-butanol and polymer respectively. The activation energy for Li^+ ion transport, E_a, can be obtained by using the Vogel–Tamman–Fulcher relation

$$\text{Activation energy}\ \sigma = \sigma_0 T^{-1/2} \exp\left(\frac{-E_a}{T - T_o}\right) \quad (4)$$

where σ is ionic conductivity, σ_o is pre-exponential factor and T_0 is glass transition temperature. It is evident from the table that composite PVdF–HFP polymer membranes possess superior physical characteristics like higher liquid uptake, porosity, and surface area. In addition, these membranes exhibit relatively low crystallinity and lower activation energy which are essential for better ionic conductivity so as to enable to use it as a prospective polymer film in energy storage device applications.

The pore sizes of the composite membranes measured to be 2.65 nm and are around 2.97 nm for the gelled membrane which is much below the actual resolution range of SEM micrograph (Fig. 4) and hence these pores are not seen apparently. Hence, Brunauer–Emmett–Teller (BET) surface area analysis has been carried out for GPM and CPM (before gelation) to measure the pore sizes and surface area of such membranes. These properties are promising one as the basic pore size requisite for the separator in lithium batteries is <1 mm and porosity is ~40% (Celgard) [27].

3.5. Morphological studies

SEM images of GPM and CPM exhibit highly interconnected networks of pores. These pores are pre-requisites for the Li^+ ion transport during the cycling. The dispersion of nano-particulate $AlO(OH)_n$ is clearly seen from Fig. 4b. It can be seen that, CPM shows good wettability (Table 1) for liquid uptake than GPMs due to the high porosity. As a result CPMs are generally expected to facilitate faster ionic transport, high ionic conductivity, low bulk impedance and high rate capability, which render them as suitable candidate for lithium ion cells of high power density.

Table 1
Physical properties of gel (GPM) and composite PVdF–HFP membranes (CPMs).

Physical properties	GPM	CPM
Liquid uptake (%)	195	204
Porosity (%)	50	55
Crystallinity (%)	16	14
Activation energy (kJ mol^{-1})	12.05	7.05
Surface area (m^2 g^{-1})	19.4	27.7

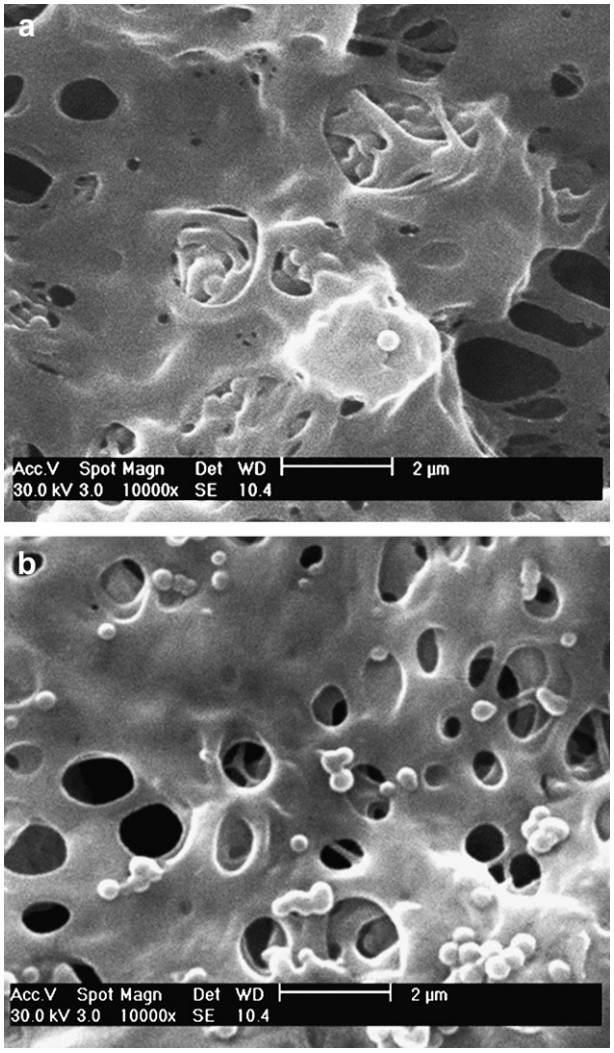

Fig. 4. SEM images of (a) gel and (b) composite PVdF–HFP membranes prepared by phase inversion.

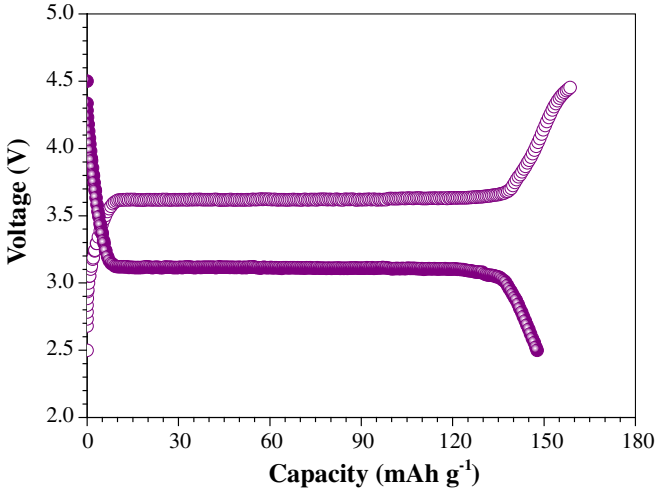

Fig. 5. Typical charge–discharge curves of Li/CPM/$LiFePO_4$ cell at C/20 rate in ambient temperature (open symbol for charge and filled symbol for discharge).

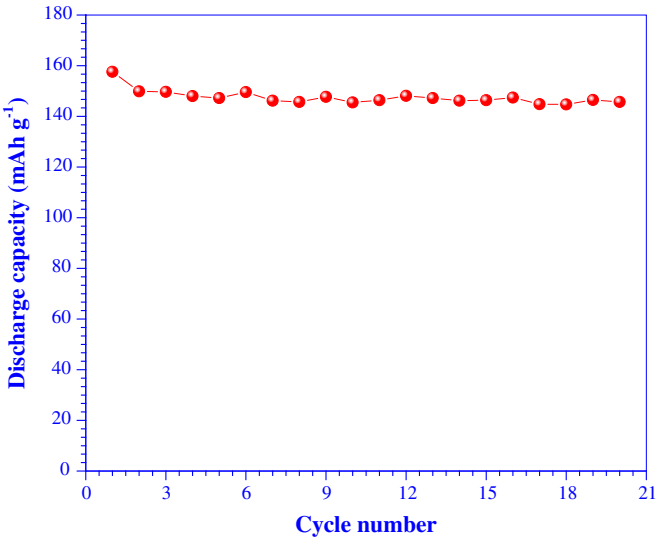

Fig. 6. Plot for discharge capacity with cycle number of Li/CPM/$LiFePO_4$ cell.

3.6. Charge–discharge studies

Jiang and Dahn [11,28–30] systematically analyzed the safety features of LiBOB with various cathode materials by accelerated rate calorimetry (ARC) studies. It was shown that, enhanced safety could be obtained with fully lithiated graphitic anode and LiBOB electrolytes. The safety concern arises when most of the tested cathode materials ($LiCoO_2$, $LiNiO_2$, $LiNi_{0.1}Co_{0.8}Mn_{0.1}O_2$, etc.) showed higher self-heating rate and reactivity with LiBOB at ambient and elevated temperatures. The $LiFePO_4$ is proven to be an exceptional one, which showed much high onset temperature in the presence of LiBOB. In this line, Dahn and co-workers [30] proposed, "thermally stable lithium ion cell" with the configuration of C/LiBOB-EC-DEC/$LiFePO_4$. In this paper, $LiFePO_4$ based Li/CPM/$LiFePO_4$ cell has been assembled to evaluate the cycling performance with composite polymer membranes.

Typical charge–discharge profile of Li/CPM/$LiFePO_4$ cell is shown in Fig. 5. It is evident that these cells show flat charge–discharge characteristics showing plateau regions around 3.6 V and 3.2 V during charge–discharge cycles. The observed profiles are very similar to that of Li/$LiFePO_4$ cells employing Celgard separator with efficiency over 95%. This shows that the polymer membrane holds good stability to act as a separator as well as a potential electrolyte. Fig. 6 shows the discharge capacity obtained from Li/CPM/$LiFePO_4$ cells with number of cycles. It is apparent that over the investigated 20 cycles, these cells exhibit stable discharge behaviour. These cells delivered a specific discharge capacity of 158 and 147 mAh g^{-1} at the second and 20th cycle discharged at C/20 rate. The cells experience a capacity fade of 0.1 mAh g^{-1} $cycle^{-1}$ over the investigated 20 cycles.

This meager capacity fade may be ascribed to the formation of solid electrolyte interphase (SEI) on the surface of electrodes. The formation of SEI (mostly consists of semicarbonates) is beneficial for the electrodes in the sense that it offsets the further unwanted reaction with the electrolyte and prevents self-discharge [31,32]. The studies vindicate that $AlO(OH)_n$ filled PVdF–HFP polymer membranes could be potentially exploited as an efficient separator cum electrolyte component in lithium batteries in conjunction with $LiFePO_4$ counterpart.

4. Conclusions

Lithium bis(oxalato)borate based composite polymer membranes were prepared by phase inversion technique with $AlO(OH)_n$ nanoparticles as fillers. The membranes were characterized through different techniques to find out their thermal stability, mechanical strength, surface morphology, porosity, ionic conductivity, etc. Incorporation of $AlO(OH)_n$ nanoparticles into the PVdF–HFP network improves the physical properties of the membranes. An attempt has been made to use these membranes as a separator cum electrolyte in a Li/$LiFePO_4$ cells. The 2016 configuration coin cells were assembled and their cycling performances have been evaluated. It is apparent that over the investigated 20 cycles, these cells exhibit stable discharge behaviour. The cells delivered a specific discharge capacity of 158 and 147 mAh g^{-1} at the second and 20th cycle discharged at C/20 rate. The cells experience a capacity fade of 0.1 mAh g^{-1} $cycle^{-1}$ over the investigated 20 cycles. The studies vindicate that $AlO(OH)_n$ filled PVdF–HFP polymer membranes could be the potential material to use as separator cum electrolyte component in lithium batteries in conjunction with $LiFePO_4$ counterpart.

Acknowledgement

One of the authors (V.A) wishes to thank Dr. Karim Zaghib, Hydro Quebec, Canada and Mrs. Anna Maria Bertasa, Solvay Solexis, Italy for kindly providing chemicals. The author is also grateful to the Council of Scientific and Industrial Research (CSIR), New Delhi for the award of Senior Research Fellowship.

References

[1] J.M. Tarascon, A.S. Gozdz, C. Schmutz, F. Shokoohi, P.C. Warren, Solid State Ionics 86–88 (1996) 49.
[2] A.M. Stephan, K.S. Nahm, Polymer 47 (2006) 5952.
[3] A.S. Aricò, P. Bruce, B. Scrosati, J.M. Tarascon, W. van Schalkwijk, Nat. Mater. 4 (2005) 366.
[4] M. Armand, J.M. Tarascon, Nature 451 (2008) 652.
[5] F. Croce, G.B. Appetecchi, L. Persi, B. Scrosati, Nature 394 (1998) 456.
[6] P.G. Bruce, B. Scrosati, J.M. Tarascon, Angew. Chem. Int. Ed. 47 (2008) 2930.
[7] B. Scrosati, Chem. Rec. 1 (2003) 171.
[8] J. Zhou, P. Fedkiw, Solid State Ionics 166 (2004) 275.
[9] Z. Florjañczyk, M. Marcinek, W. Wieczorek, N. Langwald, Pol. J. Chem. 78 (2004) 1279.
[10] B.T. Yu, W.H. Qiu, F.S. Li, G.X. Xu, Electrochem. Solid-State Lett. 9 (2006) A1.
[11] J. Jiang, H. Fortier, J.N. Reimers, J.R. Dahn, J. Electrochem. Soc. 151 (2004) A609.
[12] V. Aravindan, P. Vickraman, J. Phys. D: Appl. Phys. 40 (2007) 6754.
[13] A. Stephan, Eur. Polym. J. 42 (2006) 21.
[14] V. Aravindan, V. Senthilkumar, P. Nithiananthi, P. Vickraman, J. Renewable Sustainable Energy 2 (2010) 033105.
[15] V. Aravindan, P. Vickraman, J. Renewable Sustainable Energy 1 (2009) 023108.
[16] V. Aravindan, P. Vickraman, A. Sivashanmugam, R. Thirunakaran, S. Gopukumar, Appl. Phys. A 97 (2009) 811.
[17] Z. Li, G. Su, D. Gao, X. Wang, X. Li, Electrochim. Acta 49 (2004) 4633.
[18] C. Capiglia, Y. Saito, H. Kataoka, T. Kodama, E. Quartarone, P. Mustarelli, Solid State Ionics 131 (2000) 291.
[19] Gerard Kraus (Ed.), Reinforcement of Elastomers, Interscience, New York, 1965.
[20] V. Aravindan, P. Vickraman, Solid State Sci. 9 (2007) 1069.
[21] Z.S. Petrovic, W. Zhang, Mater. Sci. Forum 352 (2000) 171.
[22] D. Gersappe, Phys. Rev. Lett. 89 (2002) 058301.
[23] D. Shah, P. Maiti, E. Gunn, D.F. Schmidt, D.D. Jiang, C.A. Batt, E.P. Giannelis, Adv. Mater. 16 (2004) 1173.
[24] D. Shah, P. Maiti, D.D. Jiang, C.A. Batt, E.P. Giannelis, Adv. Mater. 17 (2005) 525.
[25] W. Wieczorek, J.R. Steven, Z. Florjanczyk, Solid State Ionics 85 (1996) 67.
[26] A.M. Stephan, K.S. Nahm, M.A. Kulandainathan, G. Ravi, J. Wilson, J. Appl. Electrochem. 36 (2006) 1091.
[27] P. Arora, Z. Zhang, Chem. Rev. 104 (2004) 4419.
[28] J. Jiang, J.R. Dahn, Electrochem. Solid-State Lett. 6 (2003) A180.
[29] J. Jiang, J.R. Dahn, Electrochem. Commun. 6 (2004) 39.
[30] J. Jiang, J.R. Dahn, Electrochem. Commun. 6 (2004) 724.
[31] K. Xu, S.S. Zhang, U. Lee, J.L. Allen, T.R. Jow, J. Power Sources 146 (2005) 79.
[32] K. Xu, U. Lee, S.S. Zhang, M. Wood, T.R. Jow, Electrochem. Solid-State Lett. 6 (2003) A144.